Research Article | Vol. 13, No. 4 / 1 Apr 2022 / Biomedical Optics Express 1985
Biomedical Optics EXPRESS

Fiber-laser platform for precision brain surgery

NITESH KATTA,[1,*] ARNOLDO D. ESTRADA,[2] AUSTIN B. MCERLOY,[2] AND THOMAS E. MILNER[1]

[1]Beckman Laser Institute, University of California at Irvine, East Irvine, CA 92617, USA
[2]Department of Biomedical Engineering, University of Texas at Austin, Austin, TX 78712, USA
[*]nkatta@uci.edu

Abstract: Minimally invasive neurological surgeries are increasingly being sought after for treatment in neurological pathologies and oncology. A critical limitation in these minimally invasive procedures is lack of specialized tools that allow for space-time controlled delivery of sufficient energy for coagulation and cutting of tissue. Advent of fiber-lasers provide high average power with improved beam quality (lower M^2), biocompatible silica fiber delivery, reduced cost of manufacturing, and radiant output stability over long operating periods. Despite these advancements, no fiber-laser based surgical tools are currently available for tissue resection *in vivo*. Here we demonstrate a first to our knowledge, fiber-laser platform for performing precise brain surgery in a murine brain model. In this study, our primary aims were to first demonstrate efficacy of fiber-lasers in performing precise blood-less surgery in a murine brain with limited non-specific thermal damage. Second, fiber-lasers' ability to deliver radiant energy through biocompatible silica fibers was explored in a murine brain model for blood less resection. A bench-top optical coherence tomography (OCT) guided fiber-laser platform was constructed with a stereotactic stage for performing precision brain surgery. A pulsed quasi-continuous wave ytterbium (Yb) fiber-laser (1.07 µm) was used to perform vascular specific coagulation while a pulsed nanosecond thulium fiber-laser (1.94 µm) was used to conduct bloodless cutting, all under the guidance of a swept-source OCT system centered at 1310 +/- 70 nm. Specialty linear and circular cuts were made in an *in vivo* murine brain for bloodless brain tissue resection. The two fiber-lasers were combined into a single biocompatible silica fiber to conduct brain surgery resection under the bench-top OCT system's imaging microscope. Vascular specific coagulation was demonstrated in all five mice studied. Bloodless linear cuts and point cuts were demonstrated *in vivo*. Histologically, thermal injury was measured to be less than 100 µm while a removal rate of close to 5 mm^3/s was achieved with an average Tm fiber-laser power of 15 W. To the authors' knowledge, this is the first demonstration of a fiber-laser platform for conducting *in vivo* bloodless brain tissue resection with a pulsed thulium (Tm) fiber-laser and a quasi-continuous wave (QCW) Yb fiber-laser. The demonstrated fiber-laser platform, if successfully configured for use in the operating room (OR), can provide surgeons a tool for rapid removal of tissue while making surgical resections of brain regions more precise, and can be basis for a flexible cutting tool capable of reaching hard-to-operate regions.

1. Introduction

Neurologic cancer surgery requires specialized tools that can enhance precise cutting and removal of tumor cells and tissues without damage to adjacent eloquent structures. Moreover, because neurologic cancers may be located in confined spaces adjacent to protective bony structures, damage to blood vessels results in bleeding that obscures the surgeon's visual field and must be prevented. Given the limited space available for tissue manipulation in a micro-neurosurgical procedure, numerous instruments are currently utilized for dissection followed by fragmentation and resection [1–3]. A conventional surgical approach that uses coarse cutting tools such as

#449312 https://doi.org/10.1364/BOE.449312
Journal © 2022 Received 23 Nov 2021; revised 20 Feb 2022; accepted 21 Feb 2022; published 9 Mar 2022

Biomedical Optics EXPRESS

non-specific electrocautery/ultrasonic devices in combination with limited imaging capabilities can result in damaged nerves.

Conventional surgical tools: *(1) Ultrasonic aspirators (UAs):* UAs are common debulking and resection tools (e.g., Sonopet, Stryker Inc.). UAs have a higher specificity to water-rich constituents including fibrous tissue, collagen and elastin while better sparing neural tissues [3,4]. Blood vessels, however, are not specific to UA and they fail to maintain a blood-free surgical field [3,5]. *(2) Electrocautery:* Surgeons traverse this bleeding limitation of UA by switching to an electro-cautery tool [1,5] (e.g., SILVERGlide, Stryker Inc.). However, non-specific collateral damage on the order of multiple millimeters (mms) is common [1]. Current workflow calls for switching between electrocautery and UAs resulting in longer times in the operating room (OR) while compromising neural function caused by viable tissue damage. A primary limitation in improving functional outcome is inability to preserve viable tissue (nerve function) during vascular coagulation combined with debulking/resection. Fundamentally, limitations of electrocautery and ultrasonic aspirators arise from competing requirements of hemostasis and tissue cutting or removal. Poor surgical outcomes resulting from thermal injury in adjacent neural tissues can be attributed to non-specificity of existing cautery tools to blood vessels and absence of feedback indicating successful vascular coagulation.

Lasers operating near the water absorption peak at 2 μm have received steadily increasing interest as a potential surgical device [6–9]. Interest in this wavelength range is primarily driven by the absorption properties of water near 1.94 μm and the capability of being delivered through a low-OH cost-effective silica optical fiber. Although the absorption coefficients of most soft tissues differ slightly, their absorption properties in the 2 μm spectral range are dominated by water. At this wavelength most soft tissues have absorption coefficients of 10 mm^{-1} approximately [10] corresponding to an absorption depth of approximately 100 μm. As mentioned previously [11,12], an absorption depth of 100 μm can provide an optimal balance of tissue removal rate and minimal residual thermal injury. A practical advantage of this wavelength is that low-OH biocompatible silica fibers can be used for delivery of laser energy to tissue, which is an important enabling feature for integration with existing surgical devices and workflows. Thulium-based fiber-laser systems have been demonstrated to operate efficiently at this wavelength range and offer some degree of tunability [13–16]. Thulium-doped crystal lasers and thulium-doped silica fiber-lasers have been explored for tissue ablation and have been found to provide adequate tissue removal rates (approx. 0.3 mm^3/s/W [17] with minimal residual damage [11]. Residual thermal injury can be further reduced with the use of a Q-switched thulium laser [11,18]. Although fiber based miniaturized optical systems have been presented before [19–21], none have been reported with capabilities of silica fiber delivery, high tissue removal rate, dual-wavelength blood-less resection, and able to perform soft tissue brain surgery. In this research design we demonstrate enhanced imaging and cutting using a novel surgical fiber-laser platform that combines 1) microscopic resolution of optical coherence tomography (OCT) for image guidance; with 2) vascular specific ytterbium (Yb) fiber-laser for blood vessel coagulation; and 3) precise thulium (Tm) fiber-laser for neurosurgical resection.

First, a bench-top smart laser knife system for simultaneous imaging/cutting is constructed; followed by the experimental design and procedure to investigate capabilities of the fiber-laser platform for bloodless excision of tissue in an *in vivo* murine brain model. Finally, both the vascular specific coagulation (ytterbium, Yb) and cutting (thulium, Tm) beams are combined into a single biocompatible silica fiber and *in vivo* brain tissue resection is demonstrated.

2. Materials and methods

2.1. Bench-top surgical system

A bench-top surgical system was constructed consisting of: 1) a swept source optical coherence tomography (OCT) system (1310 nm, Axsun Inc.) with a Mach-Zenhder interferometer as

Biomedical Optics EXPRESS

described previously [1]; 2) A ytterbium (Yb) fiber-laser (IPG Photonics, YLR-300/3000, λ=1.07 μm) configurable for either QCW (Quasi continuous wave, 3000 W) or CW (continuous wave, 300 W) operation used for coagulation/hemostasis; 3) A pulsed nanosecond thulium (Tm) fiber-laser (λ=1.94 μm, NUQ-1940-NA-0015F-0, Nufern, Coherent Inc.,) used for tissue resection.

The OCT system provided a longitudinal spatial resolution of 6.75 μm (in air), lateral resolution of approximately 30 μm and recorded 3D tomograms (512 × 512 × 369 voxels) with a field of view (FOV) of approximately 3.5 × 3.5 × 3 mm^3 [1]. OCT angiography (OCTA) (methods for angiography have been described previously in [1]) was carried out before and after laser coagulation/cutting processes to highlight ability to selectively and spatially target vasculature and resect tissue with adjacent tissues remaining in-tact. For blood vessel coagulation, the Yb fiber-laser was operated in QCW mode (50 μs to 200 ms programmable duration) with variable average power (max 300 W). Light emitted from the laser was collimated (IPG Photonics head) and directed onto a dichroic mirror (DM2, DMSP1500, Thorlabs Inc.,) to combine Yb and Tm beams. Spot size of the Yb fiber-laser on the sample was computed (Optical Simulation tool ZEMAX) to be approximately 120 μm. Coagulation beam size (120 μm) was selected to be larger than the Tm cutting beam size (60 μm) in order to provide a coagulation zone (twice the $1/e^2$ beam spot of Tm fiber-laser) sufficient to avoid bleeding during resection. The scanning/focusing lens was a 50 mm focal length lens (AR112-ZC-XWL-25-50, ISP Optics) working in a telecentric configuration in combination with the reflective collimator (Fig. 1) and galvanometer (GVS012, Thorlabs Inc.). For vascular coagulation, peak power limit on the Yb fiber-laser was 3000 W (10% max. duty cycle, 300 W Avg.), repetition rate and pulse duration were fixed at 100 μs depending on the temperature increase requirement and the repetition rate was adjusted to account for the 10% duty cycle (1000 Hz for 100 μs).

For tissue resection, a thulium (Tm, Nufern, NUQA-1940-NA-0015F-0)) fiber-laser was operated at 15 W average power (100 ns, 50 kHz, 300 μJ) pulse energy and followed immediately by a coagulation pulse for maintaining a bloodless surgical field. Light emitted from the laser was collimated (RC08 Thorlabs) and directed onto dichroic mirrors (DM1, DMSP1180, Thorlabs and DM2, DMSP1500 Thorlabs) to combine Tm, Yb and OCT beams. Post-procedural OCT angiography was carried out to confirm perfusion in adjacent tissue was maintained. From our previous ZEMAX and COMSOL simulations along with phantom ablation studies [12] the Tm fiber-laser provided sufficient soft-tissue ablation with varying types of cuts (point, line, square ablations) guided by OCT intensity cross-section and intensity images [12].

2.2. Biocompatible silica fiber assembly

Collimated light from both the Yb and Tm fiber-lasers were combined using a bench-top setup consisting of three XYZ micro positioners and tilt mounts (Fig. 1) consisting of a dichroic mirror (DM2, DMSP1500, Thorlabs Inc.,) and focused into a biocompatible silica fiber (Flexiva 200^{TM}, Boston Scientific, 230 μm core) via a fixed focal length parabolic reflective mirror (RC08, Thorlabs Inc, Fig. 1). Tm fiber-laser light exiting a fiber with a core size of 25 μm was coupled into a 230 μm core-diameter fiber (80–90 percent efficiency) while Yb light (50 μm fiber) was coupled into the same fiber with a slightly lower efficiency (Fig. 1(C)). The silica fiber's multimode core (230 μm diameter, numerical aperture NA 0.22 at λ=2 μm) was chosen to meet or exceed the etendue of Yb and Tm fiber-laser outputs for efficient coupling. The distal end of the fiber was fastened to another XYZ stage (XYZ with PT3, Thorlabs Inc., stage and tilt with TTR001, Thorlabs Inc., stage), adding micromanipulation capability, so that the fiber distal tip could be positioned in the field-of-view (FOV) of the OCT system (Fig. 1(B)) and near the murine brain for performing image-guided fiber ablation. No focusing optics were positioned at the output of the biocompatible silica fiber. The tip of the biocompatible silica fiber contained no distal element(s) and was a simple flat polished surface (Fig. 1(C)). During OCTA acquisition,

Biomedical Optics EXPRESS

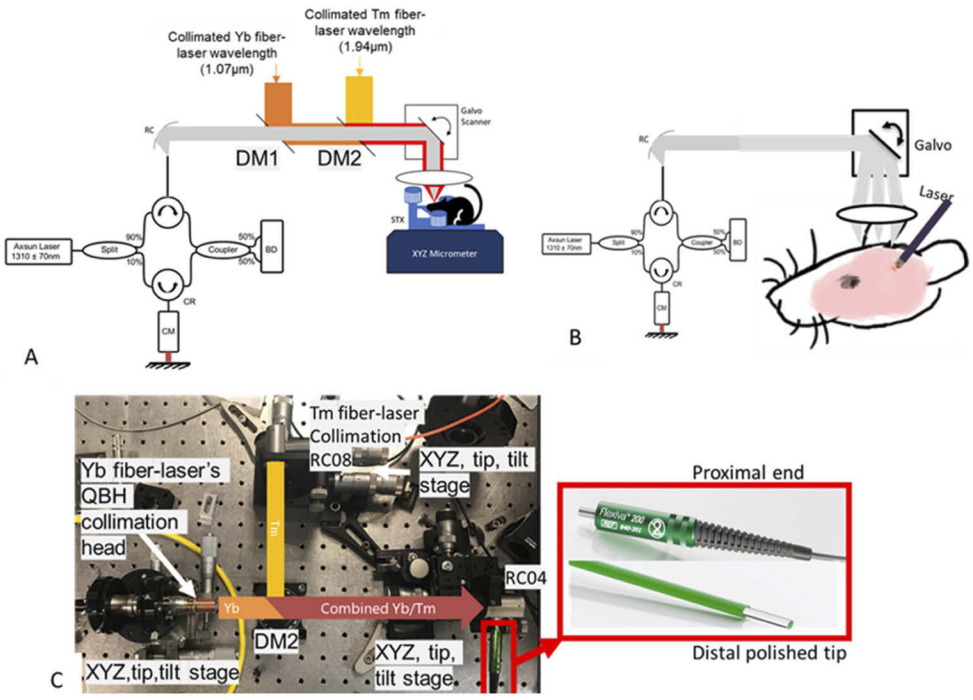

Fig. 1. A) Bench top fiber-laser platform consisting of thulium (Tm) fiber-laser combined with an Yb fiber-laser for cutting and coagulation respectively and incorporating swept source OCT image-guidance. B,C) Biocompatible silica fiber implementation of Tm/Yb fiber-laser configuration for *in vivo* murine brain surgery. Collimation of Yb fiber-laser beam utilized a QBH (quartz block head) collimator (IPG Photonics) from a 50 μm core silica fiber (0.1 NA) to a 3 mm diameter beam. Collimation of Tm fiber-laser beam utilized a reflective collimator (RC08, Thorlabs Inc). Yb and Tm beams were combined with a dichroic mirror (DM2, DMSP1500, Thorlabs Inc.) and coupled into a multimode fiber (Flexiva 200, Boston Scientific) terminating in a flat distal polished tip.

the fiber distal tip was moved out of the OCT system's FOV. The XYZ stage allowed for precise, consistent, and repeatable positioning of the fiber distal tip during OCT guided resection in the cortical regions.

2.3. Experimental animals

Mice (Harlan Labs) were anesthetized and placed onto a cranial stereotaxic stage and were administered with dexamethasone (0.02 ml at 4 mg/ml) and carprofen (4 mg/kg of a 50 mg/ml solution) intramuscularly. The scalp was then retracted to expose the bregma and the periosteum was covered with a lidocaine solution for hemostasis during scraping. The periosteum was gently scraped with a scalpel to expose the cranium and the surface dried. Using a high-speed micro-drill (0.5 mm, Stoelting Co), the cranium was thinned in a 4.5 mm diameter circumference of skull region overlying the brain area of interest and the bone was gently removed. Mice, on the stereotaxic stage, were then placed under the bench-top system for conducting surgery as described in section 2.4. Each mouse underwent craniotomy following a similar procedure. Mice were euthanized after laser surgery, brains formalin fixed, removed from the cranium, cut into coronal sections, and histologically processed as hematoxylin and eosin (H&E) stained slides. Additionally, histological sectioning was done with Nissl staining to identify any regions

Biomedical Optics EXPRESS

of thermal damage and were analyzed to study the effects on tissue caused by Tm fiber-laser ablation.

2.4. *In vivo murine brain surgery*

Laser surgery in three mice (n = 3, #C1, #C2, #C3) was completed utilizing the Yb/Tm benchtop laser surgical system. Surgical workflow consisted of a protocol starting with an initial OCT imaging step, a series of image-guided Yb coagulations, a series of image-guided Tm ablations and a post-ablation imaging step. The Yb irradiation path resulted in a laser spot size (approximately 120 µm from ZEMAX simulation) slightly larger than that for Tm (approximately 60 µm). Targeted coagulations were carried out and OCT angiography images were recorded between each step. For resection, Yb and Tm fiber-lasers were triggered and synchronized to irradiate the tissue first with an Tm laser dose (100 ns, 50 kHz, 300 µJ for a total duration of 5 ms) to achieve resection along with a time synchronized coagulation Yb pulse (75 mJ, 100 µs, 1 kHz Yb pulse train for a total 10 ms duration) to perform a post coagulation step. During resection, OCT imaging was carried out to verify and confirm blood-less resection in the field of view. Time synchronization of the pulses alongside live OCT B-scans was conducted using LabVIEW as previously reported [1,12].

Additionally, two mice (n = 2, #C4, #C5) underwent surgery with a biocompatible optical fiber implementation of the Yb/Tm dual-wavelength benchtop system (Fig. 1). Similar to the surgical workflow described above, cortical regions were selected to be first coagulated under OCT image-guidance followed by controlled Tm fiber-laser ablation. The fiber tip was maneuvered and positioned within 100 µm of the cortical tissue under live B-scan OCT image guidance.

3. Results of precise Tm/Yb ablation/coagulation with OCT guidance for *in vivo* murine brain surgery:

A region of cortical tissue (mouse #C1) was selected for Yb fiber-laser coagulation and Tm/Yb combined ablation. A pre-operative vascular network OCTA image (Fig. 2, panel A) is overlayed on the post coagulation image (Fig. 2, panel B) showing clear coagulation margins. Post-surgical ablation resulted in consistent cuts during surgery while the surgical field remained entirely bloodless (Fig. 2, panel C). Two histology slides in the vicinity of the laser cuts were obtained (Fig. 2, panels C,D and Fig. 3 panels A,B). These tissue cuts qualitatively correlated with histological tissue sections in size, shape (Fig. 2, Fig. 3) and in terms of morphology with minimal observed thermal damage. Although, OCT images show a laser modified zone of about 100 µm (Fig. 2, panel C), this is not observed in histology sections (Fig. 2, panel D). A possible explanation is that such damaged ablated regions sometimes stick to the skull and during histological processing a shrinkage of features can be observed. We do not think thermal damage in the cortex to extended beyond 100 µm, given the shallow penetration depth of the Tm fiber-laser and OCTA visualization of vascular blood flow post laser procedure near the ablated regions.

Average tissue removal rate in brain tissue was computed experimentally to be approximately 5 mm^3/s with an assumption on losses in transmission in the bench-top system (90 percent through ZEMAX optical simulation) and computed features with an assumption of a conical-shaped resection in murine brain tissue. This experimentally computed rate was similar to our previous bench-top phantom study accompanied by corresponding ZEMAX and COMSOL simulations showing a slightly higher removal rate in gelatin phantoms [12]. In another murine brain surgery (mouse #C2), tissue cutting was attempted in presence of a large blood vessel (Fig. 4, panel A, mouse #C2). Figure 4, panel A, shows an OCT angiography enface image collected before resection was attempted. The described Tm/Yb pulse scheme was implemented and surgical incision into the brain without bleeding (Fig. 4, panel C) was demonstrated maintaining a bloodless surgical field. Figure 4(B) shows the OCT angiography image collected after resection

Biomedical Optics EXPRESS

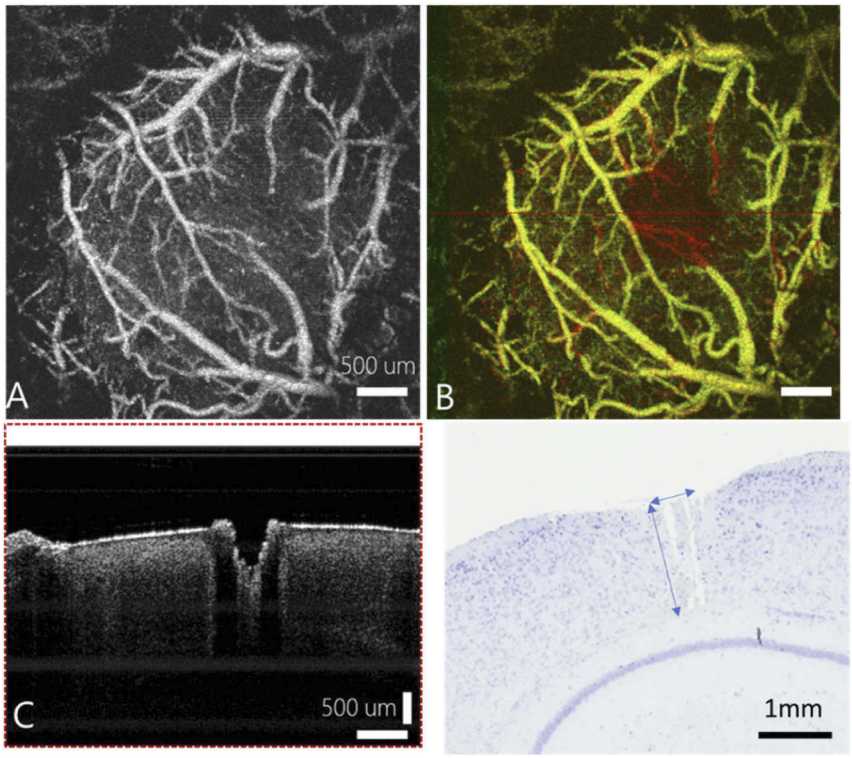

Fig. 2. A). Pre-surgery angiography of brain in control mouse #C1. B) Post surgery angiography of the control mouse #C1. C) Post surgery B-scan of ablation crater produced by Tm laser. D) Corresponding histology slice qualitatively close to B-scan OCT measurements. (note: Histological processing resulted in adjacent tissue appearing in this slide.)

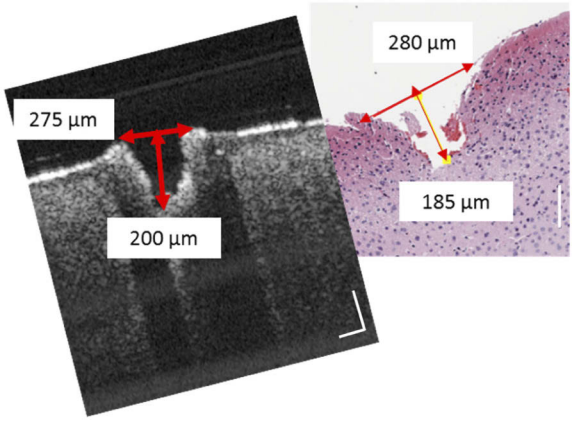

Fig. 3. Qualitative comparison of post-surgery OCT B-scan (left) and a co-registered H&E stained tissue section (right) in an adjacent location to Fig. 2 (control mouse #C1). Scale bar is 100 µm.

was carried out in the cortical region (Fig. 4, panel C). Figure 4, panel C, shows an intensity OCT cross-sectional image highlighting location of the cut and its qualitative correlation to histology (Fig. 4, panel D).

Biomedical Optics EXPRESS

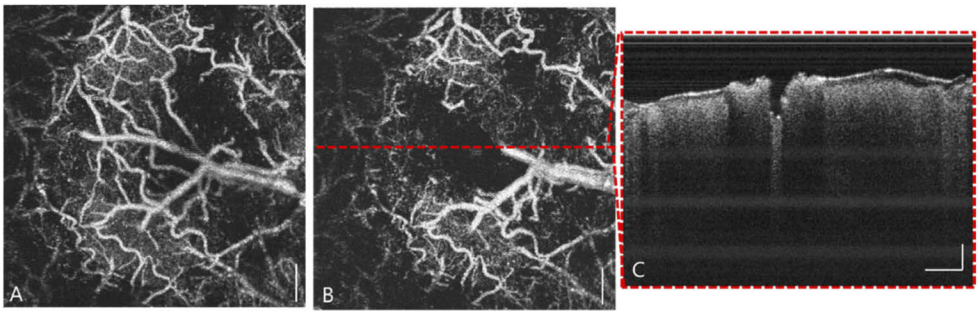

Fig. 4. A) Pre-surgery OCT murine brain angiography (mouse #C2). B) A) Post-surgery OCT murine brain angiography. C) B-scan post-surgery OCT cross-sectional images. Scale bar 500 µm

Next, *in vivo* surgical resection using a biocompatible silica fiber in close contact with the murine brain (230 µm core diameter) was attempted. For these experiments, fluence at the polished fiber distal tip was less than that in the open beam geometry (Fig. 1(A)) and resulted in successful surgical resection (Fig. 5). Figure 5, panel A, shows a pre-surgical OCT angiography (OCTA) image collected in the fiber resection geometry (Fig. 1, panel B). A post-surgery OCTA image (Fig. 5, panel B) shows details of tissue modification from laser resection compared to initial pre-surgery angiography (Panel A, Fig. 5). Panel C in Fig. 5 shows an OCT intensity cross-sectional image highlighting the resected region. The volumetric tissue removal rate in mice (#C4,5) was reduced in the fiber resection geometry and consistent with a lower fluence rate at the distal tip of the biocompatible fiber.

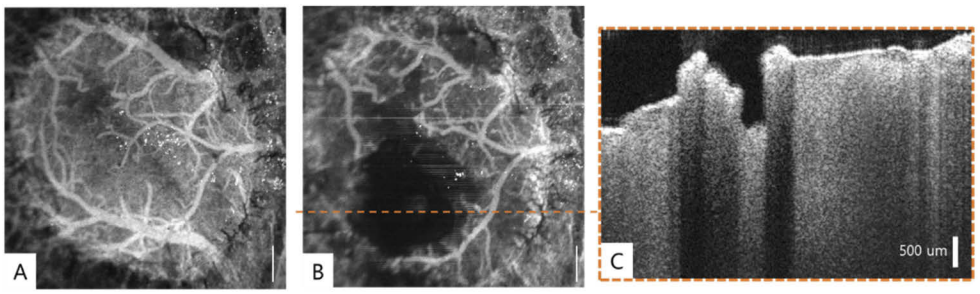

Fig. 5. *In vivo* surgery with biocompatible silica fiber implementation (see Fig. 1). A) Pre-surgical OCT angiography image B) Post surgery OCT angiography image C) B-scan OCT intensity image at dashed line in Panel B. Scale bar 500 µm.

4. Discussion and conclusions

Thulium fiber-lasers possess unique features required for rapid and precise tissue ablation. Low OH silica fiber compatibility with the Tm fiber-laser wavelength makes this source an attractive solution for a translational surgical cutting tool for consistent tissue ablation. But, given its high penetration depth, unlike Er:YAG and CO_2, cavitation and mechanical properties of different tissue types play an important role in determining ablation consistency. An advantage of OCT as described here is that most NIR/IR/Mid-IR wavelength laser-tissue interactions occur on the order of a few millimeters, given the shallow depth of penetration (due to scattering or absorption skin depth), and can be monitored or studied with OCT. Current scan rates can aid in identifying laser-tissue interactions (in the order of microseconds to milliseconds). With further improvement

Biomedical Optics EXPRESS

in scan rates, the cavitation process in the tissue (hundreds of nanoseconds to microseconds) may be studied through swept source OCT imaging. Such studies will allow further refinement of surgical lasers to maximize blood vessel coagulation and ablation efficiency while maintaining surgical structural guidance to avoid critical tissue components (like nerves, blood vessels etc). Although, *in vivo* brain surgery with thulium lasers has been reported before [22,23], none of the previous studies [22] reported a bloodless resection which is unique to the current study utilizing a dual-wavelength strategy with a pulsed nanosecond thulium laser for resection and vascular specific fiber-laser for coagulation.

Additionally, even though other miniaturized fiber based applicators have been demonstrated for hard tissue (e.g., bone) ablation using Er:YAG laser [19,21] and pulsed ultrafast lasers [20], these require specialized fibers (sapphire, fluoride, germanium) with distal optics in order to deliver mid-IR light [19,21] or maintain tight spots (<few μms) for ultrafast lasers [20]. The simplicity of power scaling and ease of coupling from fiber-lasers solves this limitation. Interestingly, although the fiber output of both wavelengths (Tm and Yb) was delivered with the same core fiber (unlike bench-top system), there was no bleeding. This suggests that our rationale for bench-top spot sizes for Tm (60 μm) and circumscribed by Yb (120 μm) was conservative. Further testing is required to confirm optimal Yb/Tm wavelengths for bloodless cutting with varying blood vessel sizes. If such a requirement exists for larger blood vessels, double clad fibers may be utilized. Fiber-lasers' etendue allows for easy termination with double clad fibers without specialized optics at the distal tip of the fiber. Finally, a structural similarity index measure (SSIM) study may be conducted to characterize the statistical correlation between OCT and histology cross-sections to better validate tissue margins.

Surgical workflow in the operating room utilizes multitude of tools (electrocautery, scissors, and ultrasonic aspirators) for performing coagulation and resection resulting in long times while procedures like electrocautery for performing coagulation induces millimeter level of tissue damage to viable regions. By combining the two functionalities into two wavelengths and combining them into a single beam path allows for performing bloodless cutting. Additionally, the low NA, high brightness of fiber-lasers allows for easy coupling into biocompatible silica fibers.

Tissue removal rate with short penetration depth lasers previously reported [1] has a computed removal rate of about 0.16mm^3/s. Recently studies have shown an enhancement in ablation rate with higher energy pulses along with irrigation setting [19]. Assuming a linear relationship with average power and taking into account the highest average power Er:YAG laser reported in the literature removal rates can be improved to about 1–2 mm^3/s. While higher removal rates are possible as reported before [19], the tissue removal rate is still limited for many practical applications in soft tissue given the need for specialized fibers (like fluoride, sapphire, germanium), irrigation and distal optics. The current demonstration of a fiber-laser platform with Tm irradiation combined with blood vessel coagulation is a solution to these limitations due to: 1) silica fiber compatibility and 2) higher average power with the advent of kW average power fiber-lasers [24–26]. A Tm/Yb combination system provides high aspect ratio ablation margins while maintaining a relatively small thermal damage zone. Compared to Er:YAG (250 μm spot size) [1], the spot size of the thulium laser irradiation for ablation was about 60 μm, allowing for a higher aspect ratio ablation (Fig. 2(C)). Limitations of Er:YAG laser for translation into the clinic are solved by the Tm/Yb fiber-laser combination for tissue ablation and coagulation. While Yb fiber-laser still provides clean coagulation, the Tm/Yb combined ablation allows for use of silica fibers to access any body cavity.

Tissue removal rate possible with the highest power Tm fiber-laser reported in the literature is computed to be much higher than 100 mm^3/s assuming a linear relationship with average power, thus becoming a viable tool for efficient and fast laser surgery. [24–26]. In our previous ZEMAX and COMSOL simulations utilizing the blow-off theory of ablation [27,28], we report a removal

Biomedical Optics EXPRESS

rate of about 30 mm^3/s may be possible with an average power of 30 W [12] which is higher than what would be the case with a linear relationship with average power. Moreover, some design improvements may be envisioned to the current system. First, use of fiber-optic signal/pump combiners and multimode fiber combiners can remove the need for complex bench-top fiber coupling optics. Secondly, in the current system the fiber tip needs to be placed close to the tissue surface to maintain tissue removal. Alternative configurations of lensed tips can allow different working distances between the fiber tip and tissue surface. Finally, alternative wavelengths in the 900–1000 nm spectral range may provide enhanced blood coagulation capabilities compared to 1070 nm.

In conclusion, novel capabilities are incorporated in a single device by: 1) overcoming competing requirements of hemostasis and cutting by a dual-wavelength approach; 2) rapid coagulation of blood vessels with a blood specific laser wavelength [27,28]; 3) maintaining a blood-free surgical field during cutting of a selected tissue region; and 4) integration of a biocompatible fiber into a small footprint, simple micro-neurosurgical applicator. If successfully configured for use in the OR, such a device can provide surgeons a tool for rapid removal of tumors while making surgical resection of tissue more precise, improving patient outcomes and prognosis with shorter procedure times.

Funding. Clayton Foundation for Research; Cancer Prevention and Research Institute of Texas (Grant Number: CPRIT-DP150102).

Acknowledgments. The authors would like to acknowledge the Cancer Prevention Research Institute of Texas (CPRIT) and the Clayton Foundation for research for providing support in conducting the research. Additionally, the authors would like to thank Dr. Peyman Ahmadi for insightful discussions on the capabilities of the thulium (Tm) fiber-laser.

Disclosures. The authors declare no conflicts of interest

Data availability. Data underlying the results presented in this paper are not publicly available at this time given the large size of the raw OCT data sets and may be obtained directly from the authors upon reasonable request.

References

1. N. Katta, A. D. Estrada, A. B. Mcelroy, A. Gruslova, M. Oglesby, G. Cabe, M. D. Feldman, R. Y. D. Fleming, A. J. Brenner, and T. E. Milner, "Laser brain cancer surgery in a xenograft model guided by optical coherence tomography," Theranostics **9**(12), 3555–3564 (2019).
2. N. Sanai and M. S. Berger, "Glioma extent of resection and its impact on patient outcome," Neurosurgery **62**(4), 753–766 (2008).
3. F. G. Barker and S. M. Chang, "Improving resection of malignant glioma," Lancet Oncol. **7**(5), 359–360 (2006).
4. A. Harati, K.-M. Scheufler, R. Schultheiss, A. Tonkal, K. Harati, P. Oni, and T. Deitmer, "Clinical features, microsurgical treatment, and outcome of vestibular schwannoma with brainstem compression," Surg. Neurol. Int. **8**(1), 45 (2017).
5. J. E. Kennedy, "Innovation: High-intensity focused ultrasound in the treatment of solid tumours," Nat. Rev. Cancer **5**(4), 321–327 (2005).
6. G. Wendt-Nordahl, S. Huckele, P. Honeck, P. Alken, T. Knoll, M. S. Michel, and A. Häcker, "Systematic evaluation of a recently introduced 2-µm continuous-wave thulium laser for vaporesection of the prostate," J. Endourol. **22**(5), 1041–1046 (2008).
7. N. M. Fried and K. E. Murray, "High-power thulium fiber laser ablation of urinary tissues at 1.94 µm," J. Endourol. **19**(1), 25–31 (2005).
8. S.-J. Xia, J. Zhuo, X.-W. Sun, B.-M. Han, Y. Shao, and Y.-N. Zhang, "Thulium laser versus standard transurethral resection of the prostate: a randomized prospective trial," Eur. Urol. **53**(2), 382–390 (2008).
9. T. De Boorder, ÃL Waaijer, and P. J. Van Diest, "Ex vivo feasibility study of endoscopic intraductal laser ablation of the breast," Lasers. Surg. Med. **50**(2), 137–142 (2018).
10. G. M. Hale and M. R. Querry, "Optical constants of water in the 200-nm to 200-µm wavelength region," Appl. Opt. **12**(3), 555 (1973).
11. A. F. El-Sherif and T. A. King, "Soft and hard tissue ablation with short-pulse high peak power and continuous thulium-silica fibre lasers," Lasers Med. Sci. **18**(3), 139–147 (2003).
12. N. Katta, A. B. McElroy, A. D. Estrada, and T. E. Milner, "Optical coherence tomography image-guided smart laser knife for surgery," Lasers Surg. Med. **50**(3), 202–212 (2018).
13. F. Stutzki, F. Jansen, C. Jauregui, J. Limpert, and A. Tünnermann, "2.4 mJ, 33 W Q-switched Tm-doped fiber laser with near diffraction-limited beam quality," Opt. Lett. **38**(2), 97 (2013).

Biomedical Optics EXPRESS

14. T. Walbaum, M. Heinzig, F. Beier, A. Liem, T. Schreiber, R. Eberhardt, and A. Tünnermann, "Spatially resolved measurement of the core temperature in a high-power thulium fiber system," Proc.SPIE 9728, 97280 (2016).
15. L. Shah, R. A. Sims, P. Kadwani, C. C. C. Willis, J. B. Bradford, A. Pung, M. K. Poutous, E. G. Johnson, and M. Richardson, "Integrated Tm:fiber MOPA with polarized output and narrow linewidth with 100 W average power," Opt. Express **20**(18), 20558 (2012).
16. D. J. Richardson, J. Nilsson, and W. a Clarkson, "High power fiber lasers: current status and future perspectives," J. Opt. Soc. Am. B **27**(11), B63–B92 (2010).
17. P. Ahmadi, A. Estrada, N. Katta, E. Lim, A. McElroy, T. E. Milner, V. Mokan, and M. Underwood, "1940nm all-fiber Q-switched fiber laser," Proc. SPIE **10083**, 100830G (2017).
18. A. Vogel and V. Venugopalan, "Mechanisms of pulsed laser ablation of biological tissues," Chem. Rev. **103**(2), 577–644 (2003).
19. L. M. Beltrán Bernal, F. Canbaz, A. Droneau, N. F. Friederich, P. C. Cattin, and A. Zam, "Optimizing deep bone ablation by means of a microsecond Er:YAG laser and a novel water microjet irrigation system," Biomed. Opt. Express **11**(12), 7253 (2020).
20. K. Subramanian, L. Andrus, M. Pawlowski, Y. Wang, T. Tkaczyk, and A. Ben-Yakar, "Ultrafast laser surgery probe with a calcium fluoride miniaturized objective for bone ablation," Biomed. Opt. Express **12**(8), 4779–4794 (2021).
21. L. M. Beltrán Bernal, F. Canbaz, S. E. Darwiche, K. M. R. Nuss, N. F. Friederich, P. C. Cattin, and A. Zam, "Optical fibers for endoscopic high-power Er:YAG laserosteotomy," J. Biomed. Opt. **26**(09), 1–13 (2021).
22. B. Tunc and M. Gulsoy, "Stereotaxic laser brain surgery with 1940-nm Tm:fiber laser: an in vivo study," Lasers Surg. Med. **51**(7), 643–652 (2019).
23. N. Katta, A. Mcelroy, A. Estrada, and T. E. Milner, "Optical coherence tomography (OCT) guided smart laser knife for cancer surgery," Proc. SPIE 10054, 100540M (2017).
24. A. Sincore, J. D. Bradford, J. Cook, L. Shah, M. C. Richardson, L. Fellow, and A. Thulium-doped, "High average power thulium-doped silica fiber lasers : review of systems and concepts," IEEE J. Sel. Top. Quantum Electron. **24**(3), 1–8 (2018).
25. C. G. Aida, M. G. Ebhardt, T. H. Euermann, F. S. Tutzki, and C. J. Auregui, "Ultrafast thulium fiber laser system emitting more than 1 kW of average power," Opt. Lett. **43**(23), 5853–5856 (2018).
26. A. Sincore, J. Cook, D. J. Shin, P. Roumayah, N. Bodnar, and M. Richardson, "System design for a >1 kW in-band pumped thulium-doped fiber amplifier (Conference Presentation)," in *Proc.SPIE* (2019), 10897.
27. A. L. Mckenzie, "Physics of thermal processes in laser-tissue interaction," Phys. Med. Biol. **35**(9), 1175–1210 (1990).
28. M. Fawaz, N. Katta, G. Michael, and M. Thomas, "Vascular laser thermolysis of vessels varying in size in the CAM model," in *Biomedical Engineering Society* (2018), (77).